# Steady state voltage stability with AVR voltage constraint

Escola de Engenharia de São Carlos – USP, Electrical Engineering, Av. Trabalhador Sancarlense, 400, 13566-590 São Carlos, SP, Brazil

## ARTICLE INFO

## ABSTRACT

Small-signal stability analysis in a power system uses a linearized approximation of its nonlinear model to analyze its behavior when subjected to small perturbations. In this approach, there is an implicit assumption that the perturbations are small enough so the imprecisions of the linear approximation with respect to the nonlinear model remain within an acceptable range. This restricts the validity of the linearized model to a neighborhood of the equilibrium conditions under which the model was obtained. Usually, the size and shape of this neighborhood is determined by the regions in the state-space where no protective limiters are active. However, there may be situations when a relatively small perturbation drives the system to such regions, yet there is still no threat to the stable operation of the system. This paper proposes a method to find an attraction area of the system, using a linearized model with the addition of AVR and PSS output limiters, in such a way that this area includes parts of the regions of the state space where the limiters are active, therefore widening the neighborhood of the equilibrium point where stability is guaranteed. The obtained results show that this attraction area is much larger than the neighborhood defined by the region where the linearized approximation is valid, and also indicate that the linearized model, with the addition of AVR and PSS output limiters, can provide good approximations of the nonlinear system trajectories even in some parts of the regions where the limiters are active.

## 1. Introduction

Small-signal stability problems have been reported in power systems since the middle of the last century. Usually, they happen in the form of poorly damped electromechanical oscillations, and additional control loops are required to prevent these oscillation from being harmful to the system operation [1].

The most commonly used type of controller to enhance damping of these oscillations is known as power system stabilizer (PSS), which is basically a classical phase compensator [2]. Although power systems have a highly nonlinear behavior, the PSSs are designed by classical control techniques in the frequency domain, involving linearization around a nominal operating point, controller design over the linearized nominal model and *a posteriori* verification of controller performance in the closed loop nonlinear model of the system, under various operating conditions [3].

Even though this approach is still the typical industry practice, there are two major issues inherent to it, which have motivated several different proposals for new controller design procedures ([4,5] and [6] are examples). The first one is the use of a nominal model for controller design, which may represent the system behavior only during a small fraction of its daily operation, since

the operating point of power systems usually experiences large variations.

The second one (which is the main target of this paper) is the fact that power system dynamics are highly nonlinear [3], and therefore the validity of the designed linear controllers is restricted to a small neighborhood of the equilibrium point used for linearization. Although this is a well-known fact, the actual shape and size of this neighborhood is never addressed at the design stage. Usually, the verification of the validity of the designed control law, both in terms of stability and performance, is carried out after the design (via numerical simulation of the closed loop nonlinear model). If the results of this simulation match the predicted outcome of the nominal linearized model near its respective equilibrium point and are acceptable for other selected operating points as well, then the design is considered as successful.

In transient stability studies, where the nonlinear model of the power system is directly employed, the determination of the attraction area for a particular operating condition is a typical practice [7]. When it comes to small-signal stability studies in power systems, however, this issue has only recently become the focus of intensive research. Of course, stable linearized models are attractive in the whole state-space, but the question is: **In power systems, how far from an equilibrium point can the state go, so the dynamics can still be represented by the linearized model?** Another question immediately follows this one: **Is it possible for the state to go any further, without the risk of instability?**

* Tel.: +55 16 3373 9348; fax: +55 16 3373 9372.
E-mail address: ramos@sel.eesc.usp.br

These issues have sparked a number of recent investigations on several different topics related to the precision with which the linearized models can accurately represent the nonlinear behavior of the power system. As examples, [8] and [9] propose approaches assess the impact of the limiters in the automatic voltage regulator (AVR) and PSS outputs on the small-signal stability of power systems. However, these two references neglect the fact that, for these outputs to reach their ceiling limits, the system state must drift considerably away from its equilibrium point, and therefore the notion of a small-signal is not very well-defined in this case. The effect of other nonlinearities (such as the ones introduced by the network equations, for example) might be significant over the system dynamics, and therefore the precision of the linear model in describing the power system response may be affected.

As can be seen from the considerations in the previous paragraph, the two questions posed before it are quite involved. However, although this paper does not intend to provide complete answers, it aims to shed some light over them, mainly with respect to the role played by the AVR and PSS output limiters in this issue. For this purpose, Section 2 presents a nonlinear power system model, typically used in power system stability studies, and discusses the first question stated in the previous paragraph. After that, Section 3 presents a procedure that can be used to estimate the attraction area of a linearized power system model, considering the presence of output limiters in both the AVR and the PSS. The results of the application of this procedure in a case study are presented in Section 4 and used as a basis for the discussion of the second question in the previous paragraph. The main conclusions of the paper are then summarized in Section 5.

## 2. Power system modelling

Under typical assumptions, a set of nonlinear equations to model the operation of a multimachine power system can be the following:

$$\dot{\delta}_i = \bar{\omega}\omega_i - \bar{\omega} \tag{1}$$

$$\dot{\omega}_i = \frac{1}{2H_i}\left(P_{mi} - E'_{qi}(I_{Ri}\cos\delta_i + I_{Ii}\sin\delta_i)\right) \tag{2}$$

$$\dot{E}'_{qi} = \frac{1}{\tau'_{doi}}\left(E_{FDi} - E'_{qi} - (x_{di} - x'_{di})(I_{Ri}\sin\delta_i - I_{Ii}\cos\delta_i)\right) \tag{3}$$

In (1)–(3), $\delta_i$ is the rotor angle, $\omega_i$ is the rotor speed (with respect to a synchronous reference), $E'_{qi}$ is the quadrature-axis transient voltage, for $i = 1,\ldots,n$, where $n$ is the number of generators of interest, assuming that a large portion of the system was modeled as an equivalent infinite bus. Parameter $\bar{\omega}$ is the absolute value of the synchronous speed (in radians per second), and definitions for the other parameters in these equations can be found in [10] and [2].

The set of nonlinear differential equations presented above is constrained by the following algebraic equations:

$$I_{Ri} = \sum_{k=1}^{n} E'_{qk}(G_{ik}\cos\delta_k - B_{ik}\sin\delta_k) \tag{4}$$

$$I_{Ii} = \sum_{k=1}^{n} E'_{qk}(B_{ik}\cos\delta_k + G_{ik}\sin\delta_k) \tag{5}$$

$$V_{Ri} = E'_{qi}\cos\delta_i + x'_{di}I_{Ii} \tag{6}$$

$$V_{Ii} = E'_{qi}\sin\delta_i - x'_{di}I_{Ri} \tag{7}$$

$$V_{ti} = \sqrt{V_{Ri}^2 + V_{Ii}^2} \tag{8}$$

In (4),(5), $I_{Ri}$ and $I_{Ii}$ are, respectively, the real and imaginary parts of the currents injected by the generator $i$ into the transmission network, through their equivalent internal buses. In (6)–(8), $V_{Ri}$, $V_{Ii}$ and $V_{ti}$ are, respectively, the real part, imaginary part and absolute
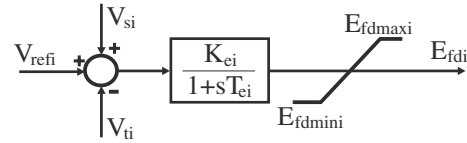


Fig. 1. Block diagram of first-order AVR with output limiters.

value of the voltage at the terminal bus of generator $i$. In this paper, a static model is used for the network and the loads are assumed as constant admittances, so they can be included in the nodal admittance matrix of the network. Parameters $G_{ik}$ and $G_{ik}$ in (4),(5) are, respectively, the real and imaginary parts of the transfer admittances between buses $i$ and $k$.

In this study, the AVR is assumed as a first-order linear regulator, whose block diagram is given in Fig. 1. In this figure, $K_e$ and $T_e$ are, respectively, the AVR gain in steady state and the AVR time constant.

It is important to highlight the presence of the windup limiters in the output of the AVR of Fig. 1. This limiter is necessary to avoid the application of excessive field voltage during relatively large disturbances in the power system operation, and is typically modelled in transient stability studies. However, the linearized models used for small-signal stability studies neglect these limiters under the assumption that the state does not drift too far away from the equilibrium point (and therefore the AVR output is within the limits).

This reasoning leads to the following conclusion (which is related to the first question of the last section): when the generator is not heavily loaded (and therefore the effect of nonlinearities is not very high in its operation), the linearized model is valid within the region where the limiters are not active. Some subjectiveness is obviously contained in the term "heavily loaded", which requires an engineering judgement to decide how much imprecision can be tolerated in the response of the linearized model with respect to the one of the nonlinear model.

However, relatively small perturbation not rarely take the generator to an operating region where the limiters are active, yet there is still no significant threat to its stable operation. The linearized model is useless in this situation because, if it is stable, then it is attractive everywhere in the state-space, so it does not provide any information on the system stability in the regions where the limiters are active. Therefore, this paper asks the following question: **using the linearized model and considering the presence of the limiters, is it possible to find a region where a stable operation of the generator is guaranteed, even when the limiters are active?** The answer is yes, and this paper will show how in the next section.

## 3. Estimating the attraction area in the presence of limiters

Before proceeding to answer the previous question, we must remind that the response of power systems to small perturbations may be oscillatory, and therefore a PSS must be designed to provide adequate damping for these oscillations, as mentioned in Section 1. Fig. 2 shows the typical block diagram of a PSS, and it
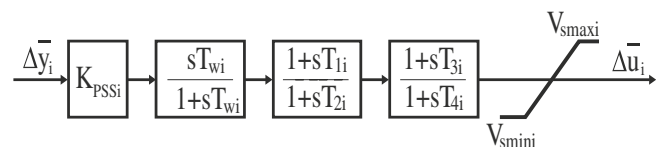


Fig. 2. Block diagram of PSS with output limiters.

is possible to see that this controller also possesses windup limiters in its output [2]. Therefore, both the AVR and PSS output limiters must be taken into account when answering the previous question.

The first step in the design of the PSS is the choice of an output signal from the power system model that exhibits good observability with respect to the oscillation modes of interest. Usually the rotor speeds of the generators are good candidates for such a signal selection. The input to the power system model is also usually chosen as the stabilizing signal $V_{si}$ added to the AVR summing junction, as seen in Fig. 1.

In the next step, Eqs. (1)–(3) are coupled with the ones represented by the block diagram in Fig. 1, and the algrebraic equations (4)–(8) are substituted in the resulting equations, so the previous set of differential-algebraic equations becomes a nonlinear state-speace representation of the power system. This nonlinear state-space is then linearized around an operating point defined by specific values of $P_{mi}$ and $V_{refi}$. The result is a linear state-space model in the form

$$\Delta\dot{\bar{\mathbf{x}}} = \bar{\mathbf{A}}\Delta\bar{\mathbf{x}} + \bar{\mathbf{B}}\Delta\bar{\mathbf{u}} \qquad (9)$$

$$\Delta\bar{\mathbf{y}} = \bar{\mathbf{C}}\Delta\bar{\mathbf{x}} \qquad (10)$$

In Eqs. (9) and (10), the state vector $\Delta\bar{\mathbf{x}}$ is composed by deviations from the equilibrium values of the states of the nonlinear model. The input $\Delta\bar{\mathbf{u}}$ is the deviation from the equilibrium values of the $V_{si}$ signals in Fig. 1, and the output $\Delta\bar{\mathbf{y}}$ is the deviation of the rotor speed of the generators from the synchronous speed.

Typical industry practices for PSS design involve a combination of phase compensation and pole placement techniques to determine the desired PSS parameters [11].. After the PSS is designed and placed in the generator, the closed loop system can be described by

$$\Delta\dot{\mathbf{x}} = \mathbf{A}_{cl}\Delta\mathbf{x} = (\mathbf{A} + \mathbf{BK})\Delta\mathbf{x} \qquad (11)$$

where

$$\mathbf{A}_{cl} = \begin{bmatrix} \bar{\mathbf{A}} & \bar{\mathbf{B}}\mathbf{C}_c \\ \bar{\mathbf{B}}_c\bar{\mathbf{C}} & \bar{\mathbf{A}}_c \end{bmatrix} \qquad (12)$$

and $\bar{\mathbf{A}}_c$, $\bar{\mathbf{B}}_c$ and $\bar{\mathbf{C}}_c$ are a state-space realization of the PSS transfer function.

In (11), the state vector $\mathbf{x}$ contains the state variables of (9) plus three other state variables referred to the PSS. Note that matrix $\mathbf{A}_{cl}$ is split in the terms $\mathbf{A}$ and $\mathbf{BK}$. This splitting is made to enable the treatment of the limiters in the analysis of the closed loop linearized system. Matrix $\mathbf{B}$ selects the field voltage deviations $\Delta E_{fdi}$ and the stabilizing signal deviations $\Delta V_{si}$ as the limited inputs and matrix $\mathbf{K}$ closes the loop by injecting the corresponding input signal into each of these variables. Matrix $\mathbf{K}$ is composed by the AVR gains $K_{ei}$ and PSS gains $K_{pssi}$, in such a way that it injects the field voltages into the differential equations of $\Delta\dot{E}'_{qi}$ and the PSS outputs into the equations of $\Delta\dot{E}_{fdi}$.

The outputs created by the term $\mathbf{K}\Delta\mathbf{x}$ in (11) are limited in such a way that

$$\Delta E_{fdmini} \leqslant \Delta E_{fdi} \leqslant \Delta E_{fdmaxi} \qquad (13)$$

$$\Delta V_{smini} \leqslant \Delta V_{si} \leqslant \Delta V_{smaxi} \qquad (14)$$

For simplicity, we will consider in this work that $\Delta E_{fdmini} = -\Delta E_{fdmaxi}$ and $\Delta V_{smini} = -\Delta V_{smaxi}$.

Going back to the question asked at the end of the last section, we are interested in discovering a region where stability of the linearized model (11) is guaranteed, even if the output limiters defined above are active. On the other hand, it is not interesting that this region is arbitrarily large because, even in a lightly loaded generator, the nonlinear behaviors become significant when operating far apart from the equilibrium point.

Therefore, our analysis must be restricted to a set of pre-determined initial operating conditions of interest, which are representative of possible outcomes from perturbations in the system equilibrium. These conditions can be selected from the initial post-fault values of the states resulting from the analysis of a contingency list, which is typical practice in the industry. These values will determine how far apart from the equilibrium the dynamics will start, and we want to know if the system will be stable even when such operating conditions lead to the activation of the output limiters. The following proposition provides a way to answer this question.

**Proposition 1.** *Given a set $\Delta\mathbf{x}_{0j}$, $j = 1,\ldots,r$ of initial conditions of interest, if there exists matrices of appropriate dimensions $\mathbf{P} = \mathbf{P}^T > \mathbf{0}$, $\mathbf{F}$, $\mathbf{G}$, $\mathbf{H}$ and diagonal matrices $\mathbf{D} = diag(D_{l,l})$ and $\mathbf{L} = diag(L_{l,l})$, $l = 1,\ldots, 2n$, such that*

$$\begin{bmatrix} \mathbf{M}_{1,1} & \mathbf{M}_{2,1}^T & \mathbf{M}_{3,1}^T \\ \mathbf{M}_{2,1} & \mathbf{M}_{2,2} & \mathbf{M}_{3,2}^T \\ \mathbf{M}_{3,1} & \mathbf{M}_{3,2} & \mathbf{M}_{3,3} \end{bmatrix} < \mathbf{0} \qquad (15)$$

$$\begin{bmatrix} \mathbf{P} & [(1 - L_{2k-1,2k-1})K_{ek}]^T \\ (1 - L_{2k-1,2k-1})K_{ek} & E_{fd\,max\,k}^2 \end{bmatrix} \geqslant \mathbf{0} \qquad (16)$$

$$\begin{bmatrix} \mathbf{P} & [(1 - L_{2k,2k})K_{pss\,k}]^T \\ (1 - L_{2k,2k})K_{psskl} & V_{s\,max\,k}^2 \end{bmatrix} \geqslant \mathbf{0} \qquad (17)$$

$$\Delta\mathbf{x}_{0j}^T\mathbf{P}\Delta\mathbf{x}_{0j} \leqslant 1, \qquad j = 1,\ldots,r \qquad (18)$$

$$\mathbf{0} \leqslant \mathbf{L} \leqslant \mathbf{I} \qquad (19)$$

*for $k = 1,\ldots,n$, where*

$$\mathbf{M}_{1,1} = \mathbf{F}(\mathbf{A} + \mathbf{BK}) + (\mathbf{A} + \mathbf{BK})^T\mathbf{F}^T \qquad (20)$$

$$\mathbf{M}_{2,1} = \mathbf{G}(\mathbf{A} + \mathbf{BK}) - \mathbf{F}^T + \mathbf{P} \qquad (21)$$

$$\mathbf{M}_{2,2} = -\mathbf{G} - \mathbf{G}^T \qquad (22)$$

$$\mathbf{M}_{3,1} = \mathbf{H}(\mathbf{A} + \mathbf{BK}) + \mathbf{B}^T\mathbf{F}^T + \mathbf{DLK} \qquad (23)$$

$$\mathbf{M}_{3,2} = -\mathbf{H} + \mathbf{B}^T\mathbf{G}^T \qquad (24)$$

$$\mathbf{M}_{3,3} = -2\mathbf{D} + \mathbf{HB} + \mathbf{B}^T\mathbf{H}^T \qquad (25)$$

*then the set $\epsilon(\mathbf{P}, 1) = \{\Delta\mathbf{x} \in \mathbb{R}^n \mid \Delta\mathbf{x}^T\mathbf{P}\Delta\mathbf{x} \leqslant 1\}$ is an estimation of the attraction area for the system (11), considering (13) and (14), and contains $\Delta\mathbf{x}_{0j}$, $j = 1,\ldots,r$.*

The proof of this proposition, together with the definition of each of the variables used in it, can be found in [12] or, alternatively, in [13 and 14]. They will not be repeated here due to space limitations. The set $\epsilon(\mathbf{P}, 1)$ is an ellipsoid centered in the origin of the linearized system (11), which corresponds to the equilibrium point of interest for the nonlinear state-space that models the power system, and is a positively invariant set, which ensures that all the system trajectories initiating within this set will remain in it for all $t > t_0$. Since $\epsilon(\mathbf{P}, 1)$ contains $\Delta\mathbf{x}_{0j}$, $j = 1,\ldots,r$, this ensures that, for all the initial conditions of interest, the generators will be stable even if the limiters are active during a significant part of the system trajectory.

Another interesting property of this proposition is that, since $\epsilon(\mathbf{P}, 1)$ contains $\Delta\mathbf{x}_{0j}$, $j = 1, \ldots,r$, it also contains the polyhedron $\mathbb{X}_0 = \mathbf{Co}\{\Delta\mathbf{x}_{01},\ldots,\Delta\mathbf{x}_{0r}\}$, where $\mathbf{Co}\{.\}$ stands for the convex hull. This means that the guarantee of stability is obtained not only for the response to the selected initial conditions $\Delta\mathbf{x}_{0j}$, $j = 1,\ldots,r$ (which, as previously stated, are representative of possible outcomes of perturbations in the system), but also for the response to any initial condition contained in the polyhedron $\mathbb{X}_0$ (which has $\Delta\mathbf{x}_{0j}$, $j = 1,\ldots,r$ as its vertices). Therefore, it becomes clear that one does not need to know precisely the initial conditions of interest in order to be able to apply this proposition. In other words,

only admissible bounds for the initial values of the state variables are required.

All conditions in (15)–(19) are Linear Matrix Inequalities (LMIs), except for (15), which contains the entry $\mathbf{M}_{3,1}$ given in (23). This entry includes the product of matrix variables $\mathbf{DL}$ in its last term, which introduces a bilinearity into (15). Although we cannot use an LMI solver to directly compute a solution to this problem, an algorithm can be devised to achieve this solution by iteratively applying an LMI solver. The algorithm is as follows [12]:

## Algorithm

- **Step 1:** Fix $\mathbf{L}$ and solve, for $\mathbf{P}$, $\mathbf{F}$, $\mathbf{G}$, $\mathbf{H}$, $\mathbf{D}$ and $\gamma$, the problem

$$\min \gamma \tag{26}$$

  subject to (15)–(17) and

$$\Delta \mathbf{x}_{0j}^{\mathrm{T}} \mathbf{P} \Delta \mathbf{x}_{0j} \leqslant \gamma, j = 1, \ldots, r; \tag{27}$$

- **Step 2:** If $\gamma > 1$, fix $\mathbf{D}$ obtained in the previous step and solve (26) subject to (15)–(17) and (27) for $\mathbf{P}$, $\mathbf{F}$, $\mathbf{G}$, $\mathbf{H}$, $\mathbf{L}$ and $\gamma$;
- **Step 3:** If $\gamma > 1$, go to **Step 1**.

With this algorithm, a fast and reliable numerical solution can be obtained for this problem by the iterative application of an LMI solver, such as SeDuMi [15], for example.

## 4. Case study

In this section, the previously described algorithm was applied to estimate the attraction area of two different power system models. In order to keep the conceptual nature of the presentation and the clarity in the explanation of the results, the first tested system was chosen as a single machine versus infinite bus (SMIB) system, whose single line diagram is shown in Fig. 3.

The values of the system parameters for the SMIB system of Fig. 3 are the following: $\omega_0 = 2\pi 60$ rad/s, $H = 5$ s, $x_d = 1.6$ p.u., $x'_d = 0.32$ p.u., $\tau'_{do} = 6$ s, $K_e = 100$ p.u./p.u., and $T_e = 0.01$ s. The values of the system parameters that define the operating point are: $P_m = 1$ p.u., $V_\infty = 1.2649$ p.u., $x_e = 0.4$ p.u., and $V_{ref} = 1.0762$ p.u. With these parameters, the equilibrium point corresponds to the following values for the state variables: $\delta_{eq} = 34.7$ degrees, $\omega_{eq} = 1$ p.u., $E'_{qeq} = 1$ p.u., and $E_{fdeq} = 0.9289$ p.u. (where the subscripts $eq$ denote equilibrium values).

Linearizing the system around the above operating point by truncated Taylor series expansion yields a linear representation of the system dynamics in the vicinity of this point. An eigenanalysis of this linear representation shows that, although stable, these dynamics exhibit a very poorly damped oscillatory behavior, given by the complex conjugate pair of eigenvalues $-0.0007 \pm j0.0738$. Therefore, a PSS must be employed to enhance the small-signal stability margin of the system. Using the procedure depicted in [11]., the following parameters were determined for this PSS: $K_{pss} = 1.5$ p.u./p.u., $Tw = 3.0$ s, $T1 = T3 = 0.70$ s, and $T2 = T4 = 0.11$ s.
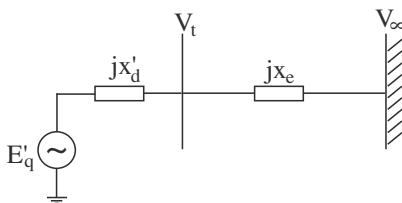


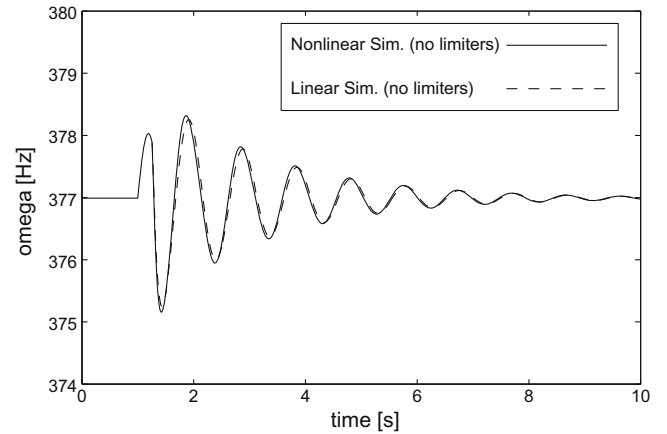**Fig. 3.** Single line diagram of the first (SMIB) tested system.



**Fig. 4.** Comparison between responses of the linearized (dashed line) and nonlinear (solid line) models – no limiters considered.

We are now faced with the following problem: although the closed loop linear model, including the designed PSS, exhibits a stable and well-damped behavior, how precise is the linear model in predicting the nonlinear behavior of the system? There is no general and definitive answer to this question, and therefore we must rely on simulation and engineering judgement to evaluate if (and where) the differences between these two representations are acceptable.

Since the linear model was produced from the nonlinear one by truncation of a Taylor series expansion, it is conceivable that these differences will become larger in those regions of the state-space which are distant from the equilibrium point around which the system was linearized. Therefore, we simulated the response of the system to a series of severe perturbations, aiming to drive the system to one of those regions. All simulations shown in the sequence were performed using MATLAB scripts.

Fig. 4 presents one of these simulations. It shows the response of the generator angular speed to a 25% drop in the infinite bus voltage $V_\infty$ and a 10% raise in the equivalent external impedance $x_e$, which might be the result of a short circuit happening somewhere in the transmission network. These faulty conditions occurred at $t = 1$ s and lasted until $t = 1.256$ s. After that, the fault is cleared and the system returns to its original configuration.

In Fig. 4, the solid line is the result of a nonlinear simulation, where the AVR and PSS output limiters were neglected. The dashed line, which is very close to the solid one, is the result obtained with the simulation of the linearized system.[1] From this figure, it is possible to conclude that, under the simulated conditions, there is no significant imprecision when using the linearized model to represent the dynamics of the nonlinear one.

Fig. 5 presents another comparison between nonlinear and linear simulations, under the same conditions of the previous simulation. This time, however, the nonlinear simulation takes the AVR and PSS output limiters into account. The limits were chosen as $\Delta E_{fdmin} = -\Delta E_{fdmax} = 5$ p.u. and $\Delta V_{smin} = -\Delta V_{smax} = 0.1$ p.u. The difference between the dashed and solid lines is evident, and we can conclude, by analyzing both Figs. 4 and 5, that this difference is entirely due to the presence of the limiters. Similar analyses for several other operating points and perturbations led to the same conclusion.

---

[1] We remark that the simulation of the linearized system is carried out only for the post-fault system, and starts at the instant of the fault clearance, when the system returns to its original configuration but the initial conditions are different from the equilibrium ones.
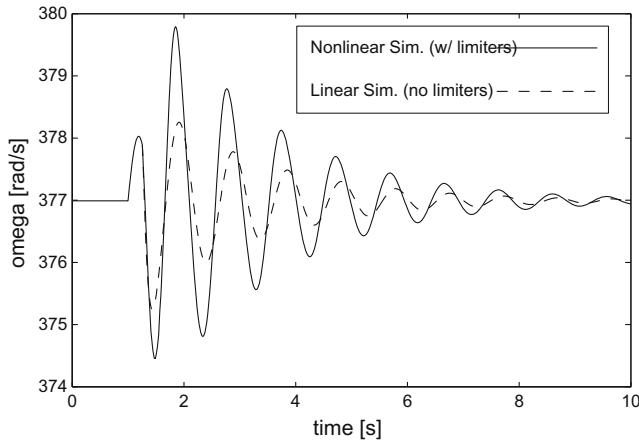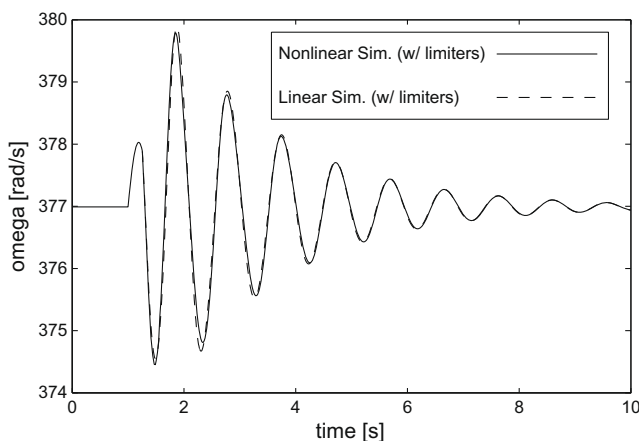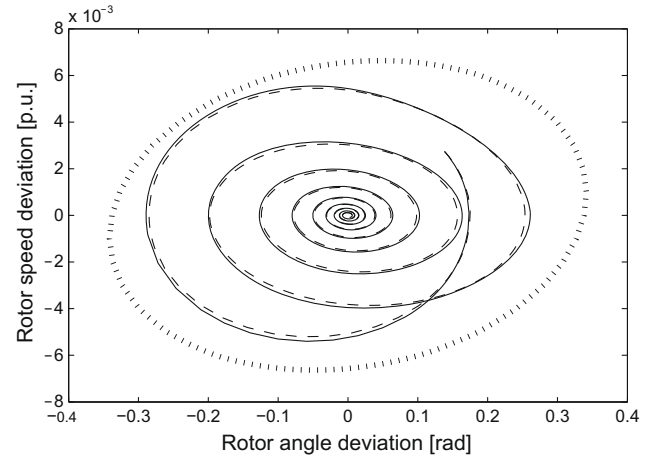
**Fig. 5.** Comparison between responses of the linearized (dashed line) and nonlinear (solid line) models – limiters in the nonlinear model.



**Fig. 7.** Estimate of the attraction area (thick dotted line) and trajectories of the linearized (dashed line) and nonlinear (solid line) models, with limiters in both models – $\Delta\delta$ versus $\Delta\omega$ plane.

The previous analysis made by comparison between Figs. 4 and 5 shows that, under the simulated conditions, the linearized model provides a good approximation of the nonlinear dynamics when the limiters are neglected, but there is significant imprecision when they are considered and the dynamics is such that leads them to be activated along the system trajectory. Due to this fact, it becomes clear that the validity of the linearized model is restricted to the region where the limiters are not active.

However, suppose that the simulated perturbation is very likely to occur in the system. If we accept the above restriction, we are left with no alternative but to perform a nonlinear simulation in order to accurately study the system behavior. On the other hand, suppose we perform a simulation of the linearized model, taking the limiters as the only nonlinear elements modelled in this simulation. Fig. 6 presents such a simulation, under the same conditions in which Figs. 4 and 5 were obtained, and compares the full nonlinear simulation results with the ones from the simulation of the linearized system, both taking the limiters into account. The dashed line is nearly unrecognizable, which shows that, for the simulated conditions, the linearized model with limiters is a good approximation of the fully nonlinear one. This was also confirmed for several other operating conditions and perturbations, and leads to the idea that we might use the linearized model with limiters to study the behavior of the nonlinear one, even in some parts of the regions where the limiters are active.

Of course, we should not expect this approach to provide good results as the system operating point drifts arbitrarily far away from the equilibrium conditions during the transient. If the operating conditions are significantly distant from the equilibrium, other nonlinearities that were discarded in the linearized model with limiters will introduce significant errors in the approximation. Another problem is that the response of the linearized model with limiters cannot be described in terms of the eigenvalues associated with the linear state-space representation of the system. Therefore, for our selected list of operating conditions and contingencies (which is commonly available at the system utilities), we would like to check if the linearized model with limiters can provide any information about the nonlinear one, and in which regions of the state-space this information can be trusted.

The algorithm presented in the previous section is particularly suited for this verification, with regard to the property of stability. To apply this algorithm, we created a contingency list containing perturbations resulting in either 25% drops or raises in the infinite bus voltage $V_\infty$, lasting for, respectively, 64, 128, 256 or 512 ms. After these periods, the fault is cleared and the system returns to its original configuration, but the initial conditions of the post-fault system are different from the equilibrium ones and cause the dynamics of the system to either start within or cross the regions where the limiters are active. The combination of the mentioned variations in $V_\infty$ and fault durations produced a total of 8 different initial operating conditions.

Using these operating conditions and applying the algorithm presented in Section 3, it was possible to find a **P** matrix[2] such that $\epsilon(\mathbf{P},1)$ is an estimate of the attraction area for the system (11), considering (13) and (14), which is the linearized model with limiters. Since we have observed in Fig. 6 that the response of the linearized model with limiters satisfactorily matches the response of the nonlinear system power system model (with the addition of the PSS), we can consider $\epsilon(\mathbf{P},1)$ as an estimate of the attraction area for this nonlinear system.

Indeed, Figs. 7 and 8 show, respectively, the projection of the set $\epsilon(\mathbf{P},1)$ over the $\Delta\delta$ versus $\Delta\omega$ plane and over the $\Delta E_q'$ versus $\Delta E_{fd}$ plane in the state space (these projections are indicated by the thick dotted lines in both figures). The conditions for the simulations shown in these figures are the same conditions of the simulations presented in Figs. 4, 6 and 5. However, to show that this



**Fig. 6.** Comparison between responses of the linearized (dashed line) and nonlinear (solid line) models – limiters in both models.

---

[2] The SeDuMi [15] and YALMIP [16] packages were used to implement the algorithm proposed in Section 3.
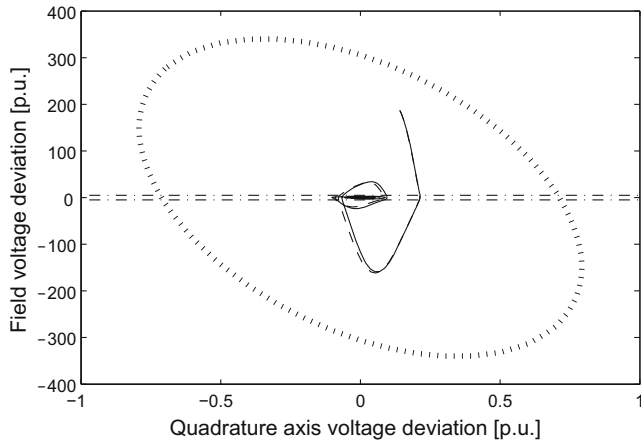
**Fig. 8.** Estimate of the attraction area (thick dotted line) and trajectories of the linearized (dashed line) and nonlinear (solid line) models, with limiters in both models – $\Delta E_q'$ versus $\Delta E_{fd}$ plane, including $\Delta E_{fd}$ limiters (dash–dotted horizontal lines).
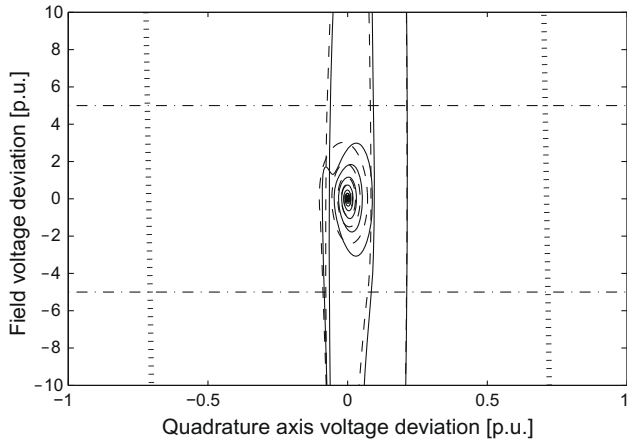


**Fig. 9.** Magnified view (centered at the origin) along the $\Delta E_{fd}$ axis of Figure 8.

estimate of the attraction area is robust with respect to differences in the initial conditions, the fault duration was modified to 200 ms.

In Fig. 8, the dash–dotted straight lines define the frontiers of the region where the AVR limiters are not active. From this figure, we can see that the obtained estimate to the attraction area is much larger than the region where the limiters are not active.[3] Therefore, as far as stability is concerned, there is a guarantee that, for the simulated conditions, the system will be stable provided that its trajectory remains within the set $\epsilon(\mathbf{P},1)$.

Zooming towards the origin of Fig. 8, we obtain Fig. 9, which shows that the dynamics of the linearized system with limiters (represented again by the dashed thin line) is a good approximation of the nonlinear system dynamics (represented by the solid thin line). This is also confirmed in Fig. 7.

Now, to demonstrate the applicability of the proposed approach to multimachine systems, a new series of tests was conducted over a 4-generator system, which is a well-known benchmark test system for small-signal stability studies and whose complete set of

data can be obtained from [2]. The single line diagram for this system is presented in Fig. 10. Generator 3 was modeled as an infinite bus, and the limits for the controller outputs in all of the other 3 generators were again chosen as $\Delta E_{fdmini} = -\Delta E_{fdmaxi} = 5$ p.u. and $\Delta V_{smini} = -\Delta V_{smaxi} = 0.1$ p.u., $i = 1,...,3$.

The contingency list for the application of the algorithm to this 4-generator system was based on the tripping, at $t = 200$ s, of the circuit brakers in the lines that connect buses 7 and 9 through bus 8, followed by the automatic reclosure of the lines, at $t = t_r$, which restores the original configuration of the system. In this second series of tests, 10 different initial conditions were generated by the variation of $t_r$ from 10 to 100 ms, in steps of 10 s.

To compare the results provided by the nonlinear and linear simulations, both considering the limiters, the same contingency mentioned in the previous paragraph was applied, this time with $t_r = 85$ ms. Fig. 11 shows the response of the rotor speed of generator 2 for both the nonlinear and linear simulations, taking the limiters into account in both cases. It is clear from Fig. 11 that the simulation of the linearized model with limiters can provide a good approximation of the response of the nonlinear model to the same contingency.

Fig. 12 shows the estimate of the attraction area for the linearized model with limiters (thick dotted ellipsoid), and the nonlinear response of the system is plotted within this estimate (solid line). The region where the limiters are active is also shown in Fig. 12 (dash–dotted horizontal lines). It is possible to see that the response of the nonlinear system actually hits the AVR output limits during the transient, so the corresponding contingency would not be considered as a small perturbation in the usual sense, yet it
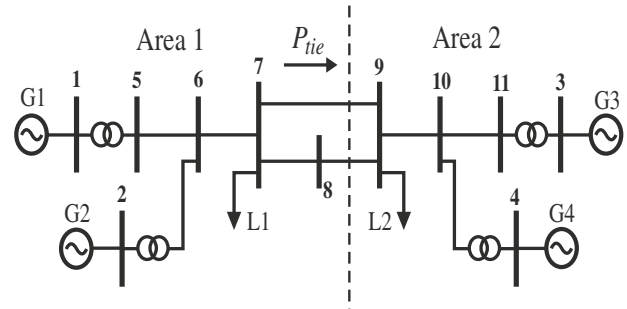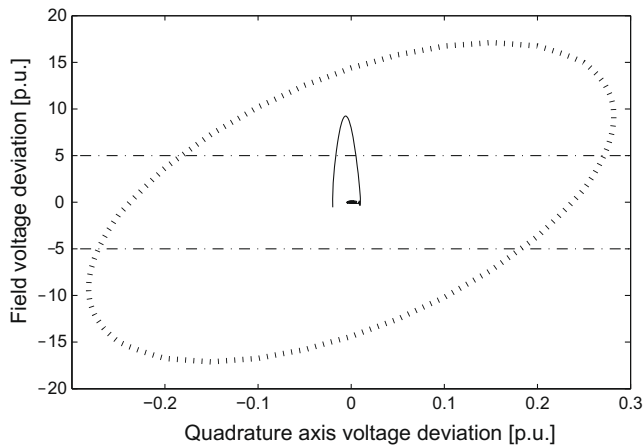


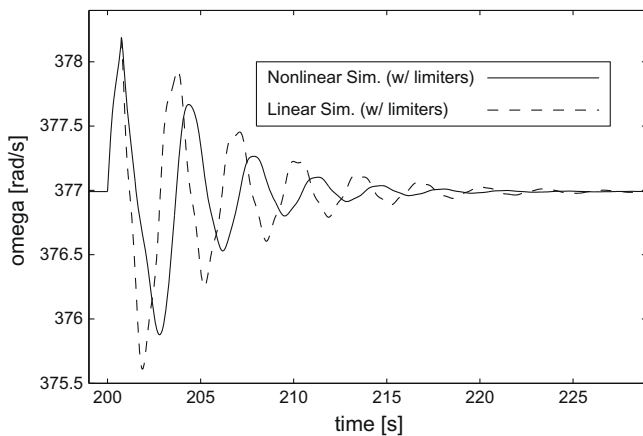**Fig. 10.** Single line diagram of the second tested system.
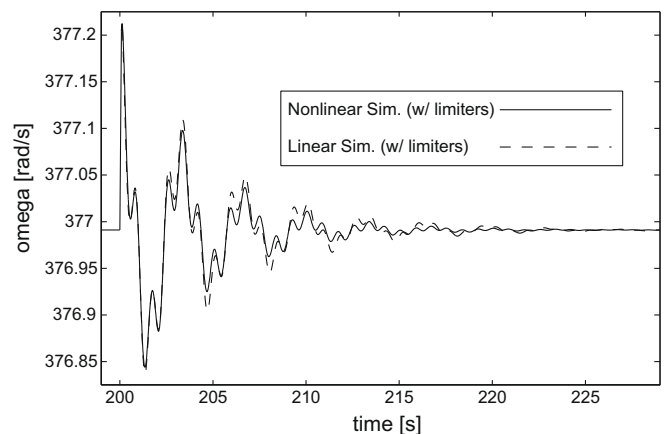


**Fig. 11.** Comparison between responses of the rotor speed of generator 2 in the linearized (dashed line) and nonlinear (solid line) models – $t_r = 85$ ms and limiters in both models.

---

[3] We must recall that, since the AVR output limits are given by windup limiters (this assumption is also made in [2]), during the period in which the system operates within the regions where the limiters are active, the actual voltage applied to the field circuit is either the upper or the lower field voltage limit, depending on which region the system is operating.

**Fig. 12.** Estimate of the attraction area (thick dotted line) and trajectory of the nonlinear (solid line) model with limiters – $\Delta E'_q$ versus $\Delta E_{fd}$ plane, including $\Delta E_{fd}$ limiters (dash–dotted horizontal lines).



**Fig. 13.** Comparison between responses of the rotor speed of generator 2 in the linearized (dashed line) and nonlinear (solid line) models – $t_r = 750$ ms and limiters in both models.

poses no threat to system stability, since it is clear from Figs. 11 and 12 that this response is stable.

To complete the analysis, Fig. 13 shows the response of the rotor speed of generator 2 to the same type of contingency used to plot the two previous figures, but this time with $t_r = 750$ ms. The initial condition for the simulation of the linearized model with limiters is now outside the calculated estimate of its attraction area, and it is clear from Fig. 13 that this linear simulation is not able to precisely represent the trajectory of the nonlinear model, even though the limiters have been taken into account. Therefore, Fig. 13 offers one more piece of evidence that the estimate of the attraction area given by the algorithm proposed in this paper can be used to distinguish between large and small perturbations in power systems.

## 5. Conclusions

In this paper, we investigated the possibility of using a linearized power system model (with the inclusion of AVR and PSS output limiters) to evaluate the stability and estimate the attraction area of the system in a particular operating condition. Several comparisons between the responses of the linearized model with limiters and of the fully nonlinear model were carried out and showed that, for the analyzed operating conditions, it is indeed possible to accurately represent the dynamics of the nonlinear model by the linearized model with the inclusion of limiters.

An algorithm to estimate the attraction area of the linearized system with limiters was proposed. Such an estimate can be useful for defining the region of safe operation for the generators, with less stringent or conservative requirements than the ones arising from the consideration that the linear models are only valid in the region where the limiters are not active.

This estimate of the attraction area provides a nice and less stringent criterion for distinguishing between large and small perturbations in power system, as opposed to the one which states that the AVR and PSS output limiters cannot be reached during the transient period for a contingency to be considered as a small perturbation. Furthermore, the possibility of representing the nonlinear system dynamics with accuracy by a linearized model with limiters is also potentially useful, since less time consuming simulations can be performed when using this linearized model with limiters. This topic, however, requires a more careful investigation, which is among the future directions of this work.

Other predicted developments of this research include the assessment of other nonlinearities that may affect the precision of the description given by the linearized model (such as machine saturation, for example) and an evaluation of the robustness of the attraction area estimates given by this approach to variations in the operating point of the power system.

## References

[1] DeMello FP, Concordia C. Concepts of synchronous machine stability as affected by excitation control. IEEE Trans Power App Syst 1969;PAS-88(4).
[2] Kundur P. Power system stability and control. New York: McGraw-Hill; 1994.
[3] Yadaiah N, Venkata Ramana N. Linearisation of multimachine power system: Modeling and control – A survey. Int J Electr Power Energ Syst 2007;29:297–311.
[4] Ramos RA, Martins ACP, Bretas NG. An improved methodology for the design of power system damping controllers. IEEE Trans Power Syst 2005;20(4):1938–45.
[5] Ramos RA, Alberto LFC, Bretas NG. Decentralized output feedback controller design for the damping of electromechanical oscillations. Int J Electr Power Energ Syst 2004;26:207–19.
[6] Ping H, Kewen W, Chitong T, Xiaoyan B. Studies of the improvement of probabilistic psss by using the single neuron model. Int J Electr Power Energ Syst 2007;29:217–21.
[7] IEEE/CIGRE joint task force on stability terms and definitions, definition and classification of power system stability. IEEE Trans Power Syst 2004;19(2):1387–1401.
[8] Xin H, Gan D D, Chung TS, Qiu J. A method for evaluating the performance of PSS with saturated input. Electr Power Syst Res 2007;77:1284–91.
[9] Xin H, Gan D, Chung TS, Qiu J. Impact of saturation nonlinearities/disturbances on power system stability: An analytical approach. Electr Power Syst Res 2008;78:849–60.
[10] Anderson PM, Fouad AA. Power system control and stability. Piscataway: IEEE Press; 1994.
[11] Larsen EV, Swann DA. Applying power system stabilizers, Parts I, II and III. IEEE Trans Power App Syst 1981;PAS-100(6).
[12] Paim C, Tarbouriech S, da Silva Jr JMG, Castelan EB. New conditions for determining stability regions for linear systems with saturating actuators. In: Proceeding of the XIV Brazilian automatic control conference, Natal, Brazil; 2002. pp. 2433–37.
[13] da Silva Jr JMG, Tarbouriech S, Garcia G. Local stabilization of linear systems under amplitude and rate saturating actuators. IEEE Trans Autom Control 2003;48(5):842–7.
[14] de Oliveira MC, Skelton RE. Stability tests for constrained linear systems. In: Moheimani SOR, editor. Perspectives in robust control. Lecture notes in control and information sciences. Springer-Verlag; 2001. p. 241–57.
[15] Sturm JF. Using SeDuMi 1.02, A MATLAB toolbox for optimization over symmetric cones; 2001. Available from: <http://sedumi.mcmaster.ca/>.
[16] Löfberg J. "YALMIP: A toolbox for modeling and optimization in MATLAB". In: Proceeding of the CACSD conference, Taipei, Taiwan; 2004. Available from: <http://control.ee.ethz.ch/~joloef/yalmip.php>.